

## Instabilities in multisero-type disease models with antibody-dependent enhancement

Lora Billings<sup>a,\*</sup>, Ira B. Schwartz<sup>b</sup>, Leah B. Shaw<sup>b</sup>, Marie McCrary<sup>a</sup>,  
Donald S. Burke<sup>c</sup>, Derek A.T. Cummings<sup>c</sup>

<sup>a</sup>Department of Mathematical Sciences, Montclair State University, Montclair, NJ 07043, USA

<sup>b</sup>US Naval Research Laboratory, Code 6792, Nonlinear Systems Dynamics Section, Plasma Physics Division, Washington, DC 20375, USA

<sup>c</sup>Johns Hopkins Bloomberg School of Public Health, Department of International Health, Baltimore, MD 21205, USA

Received 31 March 2006; received in revised form 18 October 2006; accepted 15 December 2006

Available online 28 December 2006

### Abstract

This paper investigates the complex dynamics induced by antibody-dependent enhancement (ADE) in multisero-type disease models. ADE is the increase in viral growth rate in the presence of immunity due to a previous infection of a different serotype. The increased viral growth rate is thought to increase the infectivity of the secondary infectious class. In our models, ADE induces the onset of oscillations without external forcing. The oscillations in the infectious classes represent outbreaks of the disease. In this paper, we derive approximations of the ADE parameter needed to induce oscillations and analyze the associated bifurcations that separate the types of oscillations. We then investigate the stability of these dynamics by adding stochastic perturbations to the model. We also present a preliminary analysis of the effect of a single serotype vaccination in the model.

© 2007 Elsevier Ltd. All rights reserved.

**Keywords:** Epidemics; Multisero-type; Antibody-dependent enhancement; Dengue; Vaccine

### 1. Introduction

As we become more sophisticated in our resources to fight disease, pathogens become more resilient in their means to survive. One alarming trend is the rapid evolution of new antigenic strains that stay one step ahead of vaccinations. As clearly demonstrated in influenza, it is difficult to quickly develop a vaccine that protects against the newest strain. Similarly, it can be difficult to develop one vaccine protecting against several co-circulating strains. An additional challenge is posed by viruses that exhibit antibody-dependent enhancement (ADE). This ADE effect is the increase in the viral growth rate in a secondary infection after recovery from a primary infection of a different disease serotype. Dengue and other enveloped viruses have been shown to exhibit ADE in vitro, as reported in Burke (1992) and Ferguson et al.

(1999b). Due to ADE, in theory, a vaccine developed against only one serotype could increase the infectiousness of an individual upon infection of second serotype.

The importance of understanding ADE is underscored by the pandemic status of the multisero-type disease dengue, with no vaccine available to protect against its four serotypes. Each year, tens of millions of dengue fever cases occur throughout the world. Additionally, hundreds of thousands of cases occur in a more severe form called dengue hemorrhagic fever (DHF) (CDC website, 2006). The case-fatality rate of DHF is believed to be at least 2.5% but could be reduced to 1% with proper medical treatment (WHO website, 2006). We note that DHF has been found in infections of all serotypes, but has been associated with some serotypes more than others in certain locations, and with certain strains within serotypes more than others. Overall, DHF is reported to occur more frequently among individuals experiencing a secondary infection (Nisalak et al., 2003). Therefore, administering a vaccine against one specific serotype could possibly increase the incidence of DHF.

\*Corresponding author. Tel.: +1 973 655 7812.

E-mail address: [billingsl@mail.montclair.edu](mailto:billingsl@mail.montclair.edu) (L. Billings).

Because a tetravalent dengue vaccine is not expected to become available for at least 5–10 years, the CDC urges the development of a surveillance system that provides early warning of an impending dengue epidemic (CDC website, 2006). Understanding the dynamics of a mathematical model of a multiserotype disease with ADE could help in this effort. Foundational work on ADE factors can be found in Ferguson et al. (1999a,b), Cummings et al. (2005), and Schwartz et al. (2005). Similarly, we can follow approaches used in previous dengue models without ADE, as in Esteva and Vargas (2000, 2003). Here, we examine a dynamical system with a general number of co-circulating serotypes and an ADE factor that modifies the transmissibility of secondary infections, providing derivations of and extending previous work in Cummings et al. (2005) and Schwartz et al. (2005). As we begin to understand the complexity of the dengue model, we gain a better perspective in formulating optimal vaccination strategies. Dengue has become a severe and intractable public health problem in Thailand (Nisalak et al., 2003), and we hope that models such as this will aid in the prediction and prevention of future outbreaks. While we use parameters for dengue, the model is general enough to be considered for other multistrain or multiserotype diseases.

We begin with a detailed derivation of the model in Section 2. Section 3 continues with a description of the general dynamics. A detailed analysis of the bifurcations from steady state to oscillatory dynamics is in Section 4, and the bifurcation to chaos is in Section 5. We then study the robustness of these dynamics by adding stochastic perturbations to the system in Section 6. In Section 7, we describe the effects of vaccinations against select serotypes. Finally, we discuss our results in Section 8.

## 2. Description of general $n$ -serotype model

We begin by describing the important characteristics of dengue epidemiology that we wish to model. In Southeast Asia, four serotypes of dengue have circulated for at least 50 years, while their reemergence in the Americas has been much more recent (Gubler, 1998). Primary infection with any one serotype confers immunity to that serotype but not to the others. Since tertiary infections are rare, we assume that individuals are immune to all four serotypes after two sequential serotype infections (Nisalak et al., 2003). It is also hypothesized that secondary infections carry a higher viral load, causing that person to be more infectious due to ADE (CDC website, 2006). We design our model to use these properties, but for general  $n$  serotypes so that we can evaluate the advantage of developing additional serotypes. Therefore, we follow the  $n$ -serotype susceptible-infected-recovered (SIR) model formulation, similar to the ones derived by Ferguson et al. (1999a), and limit the total number of infections to two.

We use a compartmental model assuming the population is constant, so the variables represent percentages of the

total. We denote the percentage of the population that is susceptible to all serotypes at time  $t$  by  $s(t)$ . People enter this group at a birth rate of  $\mu$ . Keeping the total population constant, we set the death rate  $\mu_d$  equal to the birth rate  $\mu$  unless otherwise noted. We assume that death is equally probable from all compartments, since dengue infection does not have a high mortality rate. Even though the rare severe form of the disease has mortality in approximately 1–5% of cases, the overwhelming majority of dengue infections do not result in death.

Dengue is transmitted by mosquito, but the time scale for transmission is sufficiently short and we assume the mosquito density is sufficiently dense that we model it by a mass action term, from person to person. The percentage of the population with a first (primary) infection by virus serotype  $i$  is represented by  $x_i(t)$ . Similarly, the percentage of the population with a secondary infection by virus serotype  $j$ , but previously recovered from serotype  $i$  ( $i \neq j$ ), is represented by  $x_{ij}(t)$ . There are  $n$  primary and  $n(n-1)$  secondary infectious groups.

The rates at which susceptibles are infected by the primary infected groups are denoted by the terms  $\beta_i s x_i$ , where  $\beta_i$  is a measure of infectivity of serotype  $i$ . We assume that the rates at which susceptibles are infected by secondary infected groups are higher because of ADE. We denote these rates in the model by the terms  $\phi_j \beta_j s x_{ij}$ , where  $\phi_j$  is the ADE factor for serotype  $j$ . The newly infected individuals move to the associated primary infected group.

People in the primary infectious groups recover at a rate of  $\sigma x_i$ . The newly recovered individuals move to the associated primary recovered group  $r_i(t)$ , which represents the percentage of the population recovered from a first (primary) infection by virus serotype  $i$ . Each primary recovered group is susceptible to all serotypes except its previous infection  $i$ . So, we model the disease transmission in a similar way to that of the susceptibles. The newly infected individuals from the primary recovered groups move to the associated secondary infected groups.

People in the secondary infectious groups recover at a rate of  $\sigma x_{ij}$  and move to one large secondary recovered group  $r_*(t)$ . This group is effectively removed from the system, since the members are now assumed to be immune to all serotypes. A description of how an individual would proceed through the model for two serotypes is shown by a flowchart in Fig. 1.

To generalize the model, we can extend the total number of serotypes to  $n$ . The number of compartments for a virus with  $n$  serotypes and two possible infections is  $n^2 + n + 2$ , including the fully recovered class. We write the general model in this compact form for  $i, j = 1, \dots, n$ :

$$\frac{ds}{dt} = \mu - s \sum_i \left( \beta_i x_i + \phi_i \beta_i \sum_{j \neq i} x_{ji} \right) - \mu_d s,$$

$$\frac{dx_i}{dt} = \beta_i s x_i + \phi_i \beta_i s \sum_{j \neq i} x_{ji} - \sigma x_i - \mu_d x_i,$$

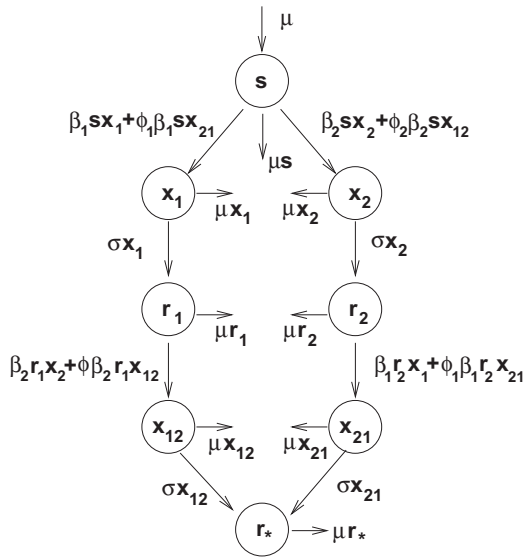


Fig. 1. A flow chart of how an individual would proceed through the model for two serotypes. Notice that the ADE factors ( $\phi_i$ ) increase the infectivity of the groups on the secondary infected level. Natural death terms are also included for all compartments.

$$\begin{aligned} \frac{dr_i}{dt} &= \sigma x_i - r_i \sum_{j \neq i} \left( \beta_j x_j + \phi_j \beta_j \sum_{k \neq j} x_{kj} \right) - \mu_d r_i, \\ \frac{dx_{ij}}{dt} &= \beta_j r_i x_j + \phi_j \beta_j r_i \sum_{k \neq j} x_{kj} - \sigma x_{ij} - \mu_d x_{ij}, \\ \frac{dr_*}{dt} &= \sum_{i,j(i \neq j)} \sigma x_{ij} - \mu_d r_*. \end{aligned} \quad (1)$$

We can also generalize the total possible number of infections an individual can contract up to  $n$ . The number of equations for  $n$  serotypes and  $n$  infections would increase to

$$2 + n! + 2 \sum_{m=1}^{n-1} \frac{n!}{(n-m)!} \quad (2)$$

if we continued to record the order of serotype infection and include the fully recovered class. In this case, it would be more efficient to form an index-set notation of previous infections, similar to the approach of [Andreasen et al. \(1997\)](#).

Notice that the ADE factors increase the infectivity of the groups on the secondary infected level. They are represented by the parameters  $\phi_i$  for  $i = 1, \dots, n$ , so that  $\phi_i > 1$ . This is in contrast to previous models describing the effect of cross-immunity, or the decrease in susceptibility for recovered individuals. Also, cross-immunity factors are bounded between zero and one, since they decrease susceptibility. Detailed studies of these systems can be found in [Castillo-Chavez et al. \(1989\)](#), [Andreasen et al. \(1997\)](#), [Dawes and Gog \(2002\)](#), and [Abu-Raddad and Ferguson \(2005\)](#). While the steady states and reduced system analysis for the general cross-immunity model are

similar to the ADE model, the ADE model exhibits interesting oscillatory and desynchronization behavior that is not found in cross-immunity model. For completeness, we continue with a description of the basic features of the general system in Eq. (1).

### 3. General dynamics of the system

The known steady states of Eq. (1) can be described as disease free and endemic equilibria. The disease free equilibrium is the trivial case where no disease is present. The entire population is susceptible, and all other compartments are empty. Its stability is determined by the basic reproduction number, or the maximum of the spectrum of the associated next generation matrix. We can define the basic reproduction number for each serotype as

$$R_i = \frac{\beta_i}{\mu + \sigma}, \quad (3)$$

resulting in a basic reproduction number for the system of  $R_0 = \max_{i=1, \dots, n} R_i$ . When  $R_0 > 1$ , the disease free equilibrium is unstable. Note that this value does not depend on the ADE factor.

There are other boundary equilibria, defined by the die out of one or more serotypes. For example, we analyze the other cases for  $n = 2$ . The equilibrium that represents the survival of serotype 1 and the die out of serotype 2 is

$$\begin{aligned} (s, x_1, x_2, r_1, r_2, x_{21}, x_{12}) \\ = \left( \frac{\sigma + \mu}{\beta_1}, \frac{\mu(\beta_1 - \sigma - \mu)}{\beta_1(\sigma + \mu)}, 0, \frac{\sigma(\beta_1 - \sigma - \mu)}{\beta_1(\sigma + \mu)}, 0, 0, 0 \right). \end{aligned} \quad (4)$$

Note that this boundary equilibrium does not depend on the ADE factor. For the stability analysis, we evaluate the Jacobian of the system at the boundary equilibrium to find the following set of eigenvalues:

$$\left\{ -\mu, -\sigma - \mu, -\frac{\beta_1 \mu}{\mu + \sigma}, \frac{-\beta_1 \mu \pm \sqrt{\beta_1^2 \mu^2 - 4\mu(\sigma + \mu)^2 \omega}}{2(\sigma + \mu)}, \frac{(\sigma + \mu)^2(\beta_2 - \beta_1) + \beta_2 \sigma \phi_2 \omega}{\beta_1(\sigma + \mu)} \right\}, \quad (5)$$

with  $\omega = \beta_1 - \mu - \sigma$ . The equilibrium is stable for parameters that keep all eigenvalues negative or have negative real part. This is true when  $R_1 > 1$  and

$$R_2 < \frac{R_1}{1 + (\sigma \phi_2 / (\sigma + \mu))(R_1 - 1)}, \quad (6)$$

as defined in Eq. (3). A similar analysis can be performed for the remaining boundary equilibrium, when only serotype 2 survives. In the symmetric case with  $R_1 = R_2$  (or  $\beta_1 = \beta_2$ ), neither boundary equilibrium will ever be stable.

If the disease free equilibrium and both boundary equilibria are unstable, then there exists a nonzero equilibrium, which we call the endemic equilibrium. In the cases of  $n > 2$ , we can consider the event of one or more serotypes dying out as the reduced nonzero endemic cases for a system with the surviving serotypes. We continue the next section with an analysis of the stability of the endemic equilibrium for a general  $n$  serotypes.

#### 4. The endemic equilibrium

We analyze the symmetric case, defined by setting the contact rates and ADE factors of all the serotypes equal ( $\beta_i = \beta$  and  $\phi_i = \phi$ , for  $i = 1, \dots, n$ ) and the death rate equal to the birth rate ( $\mu_d = \mu$ ). Using the parameters listed in Table 1 and  $n = 4$ , Fig. 2 plots the extrema of a time series of length  $t = 100$  years over a range of  $\phi$ . Here, the disease free and boundary equilibria are not stable. As  $\phi$  increases, trajectories change from converging to stable endemic equilibrium to complicated oscillatory dynamics. We numerically approximate that a Hopf bifurcation occurs at  $\phi \approx 1.88333$ , where the endemic equilibrium loses stability.

Table 1  
Model parameters

Parameter	Value	Reference
$\mu$ , 1/host life span, years <sup>-1</sup>	0.02	Ferguson et al. (1999a)
$\beta$ , transmission coefficient, years <sup>-1</sup>	400	Ferguson et al. (1999b)
$\sigma$ , recovery rate, years <sup>-1</sup>	100	Ferguson et al. (1999a)
$\phi_i$ , ADE factor of serotype $i$	1–5	–

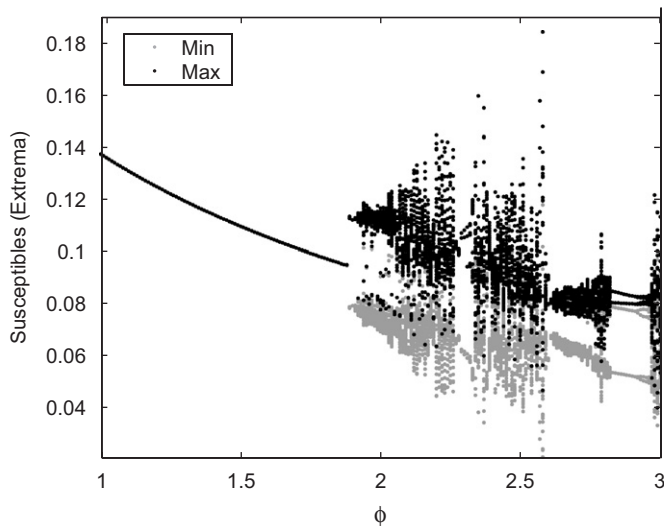


Fig. 2. A bifurcation diagram for the symmetric case of Eq. (1) with  $n = 4$ . Shown is a Poincaré section constructed from the extrema of a time series for susceptibles of length  $t = 100$  years after a transient of  $t = 5000$  years. The minima are denoted by grey points and the maxima are overlaid in black points.

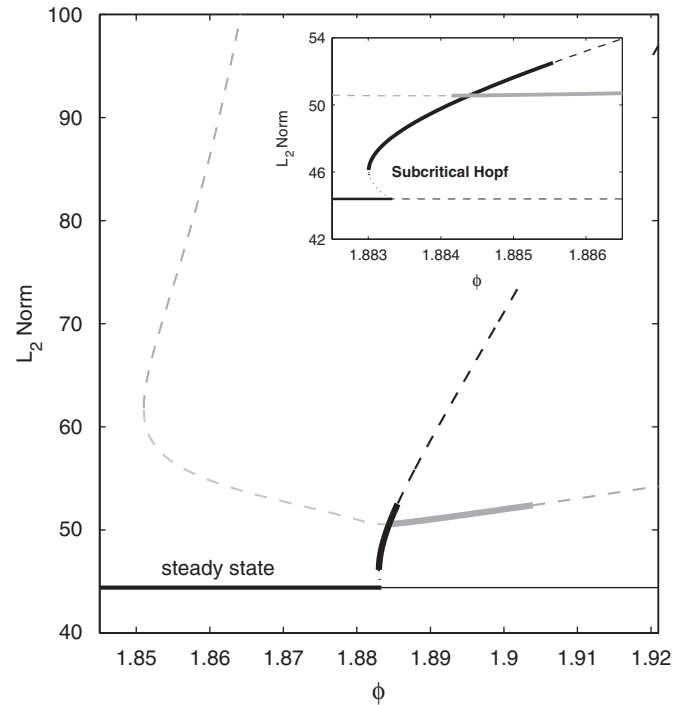


Fig. 3. A stability diagram of the periodic orbits of Eq. (1) with  $n = 4$  as a function of  $\phi$  near the Hopf bifurcation. We plot the  $L_2$  norm of the orbits and denote the stable parameter regions by the thick solid curves. See text for details.

When the endemic equilibrium is stable, the model dynamics are symmetric. All primary infectious, primary recovered, and secondary infectious variables are equal within their own classes. For a small window of  $\phi$  beyond the Hopf bifurcation, the symmetry continues in a period doubling bifurcation pattern leading to chaos. We show the transition from steady state to oscillations by numerically approximating the  $L_2$  norm of the orbits<sup>1</sup> in Fig. 3. The steady state is represented by the black curve along the bottom of the graph. Notice that the Hopf bifurcation is subcritical, since the unstable periodic orbit collides with the steady state as the steady state loses stability. See the inset for a close-up of the bifurcation. The unstable periodic orbit originates from a saddle-node bifurcation, shown by its connection to another thick black stable branch. There is a co-existing periodic orbit overlaid in grey. As the primary branch of the Hopf bifurcation loses stability at  $\phi \approx 1.8857$ , trajectories approach the grey stable periodic orbit through a hysteresis-type bifurcation. As  $\phi$  increases, the co-existing grey periodic orbit undergoes a period doubling route to chaos. The periods of the orbits are plotted in Fig. 4.

Using the symmetry between serotypes, we can reduce the symmetric  $n$ -serotype system in Eq. (1) to analyze the endemic equilibrium and Hopf bifurcation. First, set

<sup>1</sup>The  $L_2$  norm for an orbit  $\mathbf{z}(t)$  over period  $p$  is defined as  $(1/p \int_0^p \mathbf{z}(t)^T \mathbf{z}(t) dt)^{1/2}$ .

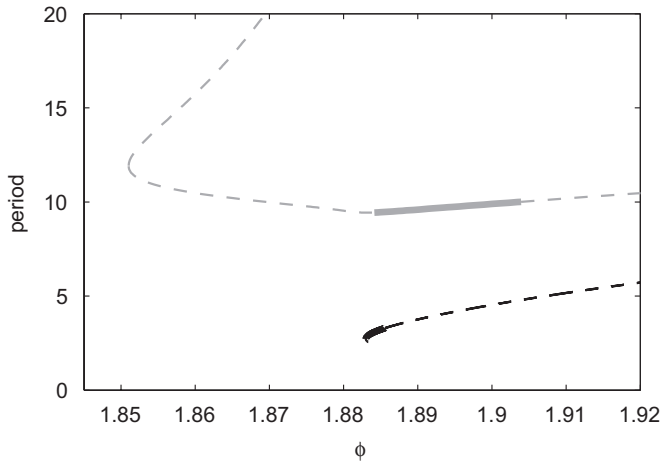


Fig. 4. A graph of the periods (in years) of Eq. (1) with  $n = 4$  as a function of  $\phi$  near the Hopf bifurcation. The thick parts of the curves denote the ranges where those periodic orbits are stable.

the variables in each of the classes equal to define the variables of a new reduced system: susceptible  $y_1 = s$ , primary infectious  $y_2 = x_i$ , primary recovered  $y_3 = r_i$ , and secondary infectious  $y_4 = x_{ij}$ , for  $i, j = 1, \dots, n$ . For  $n$  serotypes, the associated reduced model is

$$\begin{aligned} \frac{dy_1}{dt} &= \mu - n\beta y_1 y_2 - n(n-1)\beta\phi y_1 y_4 - \mu_d y_1, \\ \frac{dy_2}{dt} &= \beta y_1 y_2 + (n-1)\beta\phi y_1 y_4 - \sigma y_2 - \mu_d y_2, \\ \frac{dy_3}{dt} &= \sigma y_2 - (n-1)\beta y_3 y_2 - (n-1)^2 \beta\phi y_3 y_4 - \mu_d y_3, \\ \frac{dy_4}{dt} &= \beta y_3 y_2 + (n-1)\beta\phi y_3 y_4 - \sigma y_4 - \mu_d y_4. \end{aligned} \quad (7)$$

There is a nice agreement between the full and reduced system for values of  $\phi$  near one. In both systems, the steady state loses stability through a Hopf bifurcation. The limit cycles in the full system quickly increase in period and become unstable. The limit cycles in the reduced system do not lose stability, and in comparison, their extrema bound the full system. Therefore, we will use the reduced system to analyze only the Hopf bifurcation, and not the chaotic regime for larger values of  $\phi$ .

To analyze the destabilization of the endemic equilibrium, one would ideally linearize about the fixed point and derive the spectra as a function of  $\phi$ . Due to the length and complexity of a direct calculation of the eigenvalues for this system, we approach the analysis using perturbation theory.<sup>2</sup> A small parameter can be introduced by noticing the following. The parameter  $\mu = 0.02 \text{ year}^{-1}$  is small compared to the parameters  $\sigma$  and  $\beta$ , since  $\sigma$  and  $\beta$

are both  $\mathcal{O}(1/\mu)$ . Therefore, we rescale the parameters in relation to  $\mu$  by letting  $\beta = \beta_0/\mu$ , and  $\sigma = \sigma_0/\mu$ , where we assume  $\beta_0$  and  $\sigma_0$  are on the order of unity. We also remove the mortality terms in each of the differential equations of the reduced system by setting  $\mu_d = 0$ . Since they are originally of  $\mathcal{O}(\mu)$ , they will be small and have a negligible effect on the steady states.

The rescaled reduced system has the form

$$\begin{aligned} \frac{dy_1}{dt} &= \mu - \frac{1}{\mu} n\beta_0 y_1 y_2 - \frac{1}{\mu} n(n-1)\beta_0 \phi y_1 y_4, \\ \frac{dy_2}{dt} &= \frac{1}{\mu} \beta_0 y_1 y_2 + \frac{1}{\mu} (n-1)\beta_0 \phi y_1 y_4 - \frac{1}{\mu} \sigma_0 y_2, \\ \frac{dy_3}{dt} &= \frac{1}{\mu} \sigma_0 y_2 - \frac{1}{\mu} (n-1)\beta_0 y_3 y_2 - \frac{1}{\mu} (n-1)^2 \beta_0 \phi y_3 y_4, \\ \frac{dy_4}{dt} &= \frac{1}{\mu} \beta_0 y_3 y_2 + \frac{1}{\mu} (n-1)\beta_0 \phi y_3 y_4 - \frac{1}{\mu} \sigma_0 y_4 \end{aligned} \quad (8)$$

and yields the following steady state endemic equilibrium:

$$\begin{aligned} (y_1, y_2, y_3, y_4) \\ = \left( \frac{\sigma_0}{\beta_0(\phi+1)}, \frac{\mu^2}{n\sigma_0}, \frac{\sigma_0}{\beta_0(n-1)(\phi+1)}, \frac{\mu^2}{n(n-1)\sigma_0} \right). \end{aligned} \quad (9)$$

We would like to find where the Hopf bifurcation occurs as a function of  $\phi$  and  $n$ . We do this by evaluating the stability of the steady state solution through linearization. Therefore, we take the Jacobian of the vector field of the reduced model about the endemic steady state, and examine the characteristic polynomial for the eigenvalues. The characteristic polynomial is given by

$$F(z) = c_4 z^4 + c_3 z^3 + c_2 z^2 + c_1 z + c_0, \quad (10)$$

where the polynomial coefficients are given by  $c_0 = \beta_0^2(n-1)(\phi+1)^2/n$ ,  $c_1 = 2\beta_0^2\mu(n-1)(\phi+1)^2/\sigma_0 n + \beta_0\sigma_0/\mu$ ,  $c_2 = \beta_0^2\mu^2(n-1)(\phi+1)^2/\sigma_0^2 n + \beta_0((3n-1)(\phi+1) - \phi)/n$ ,  $c_3 = \beta_0\mu(2n-1)(\phi+1)/\sigma_0 n + \sigma_0/\mu$ ,  $c_4 = 1$ .

Since the coefficients  $c_1$  and  $c_3$  contain terms of order  $1/\mu$ , we define a rescaled function as

$$\hat{F}(z) = \mu F(z), \quad (11)$$

in which the coefficients are now given by  $\mu c_i$ ,  $i = 0, \dots, 4$ . This, in turn, allows us to apply regular perturbation theory, and we assume the solutions to Eq. (11) are of the form

$$\lambda_i = z(\mu) = z_0 + z_1\mu + \mathcal{O}(\mu^2). \quad (12)$$

The second order approximation of the eigenvalues are

$$\lambda_1 = -\frac{\beta(n-1)(\phi+1)^2\mu}{n\sigma},$$

<sup>2</sup>We note that Abu-Raddad and Ferguson (2005) recently derived recursion formulas for an endemic equilibrium in a similar cross-immunity system, and that approach might be possible for this ADE model.

$$\lambda_{2,3} = \frac{\beta\mu((n-1)\phi^2 - n\phi - n)}{2n\sigma} \pm \left(1 + \frac{\beta((n-1)(3(n-1)\phi^4 + 2(3n-4)\phi^3 - 2(n+2)\phi^2) - n^2(\phi+1)^2)\mu}{8n^2\sigma^2}\right) \sqrt{\beta\mu i}. \tag{13}$$

To determine the magnitude of the fourth eigenvalue, we notice from the characteristic polynomial coefficients that the solution must have one root which is of order  $1/\mu$ . Therefore, we define a rescaled function

$$G(z) = \mu^3 \hat{F}(z/\mu), \tag{14}$$

and again consider perturbation theory. The analysis yields a solution to  $G(z) = 0$  of  $z_0 = -\sigma_0$  for zeroth order, and the first order term is computed to be zero. Changing back to the original variables, the fourth eigenvalue can be approximated by a large negative value  $\lambda_4 = -\sigma$ .

Considering all four eigenvalues of the system, we notice that  $\lambda_1$  and  $\lambda_4$  are always negative for  $n > 1$  and our parameters. Therefore, the real part of the complex conjugate pair of eigenvalues determines the stability of the endemic equilibrium. We can approximate the location of the Hopf bifurcation by setting the real part of  $\lambda_{2,3} = 0$ . Solving for  $\phi$ , we find the boundary curve

$$\phi = \frac{n + \sqrt{n(5n-4)}}{2(n-1)}, \tag{15}$$

which is graphed in Fig. 5. Below the curve, the real part of  $\lambda_{2,3} < 0$  and the endemic equilibrium is stable. Above the curve, the endemic equilibrium is unstable and solutions oscillate. We can see that as the number of serotypes increases, the amount of ADE needed for oscillating solutions (outbreaks) decreases. The change in the Hopf point decreases as the number of serotypes increases, and the value of  $\phi$  limits to  $(1 + \sqrt{5})/2$  as  $n$  approaches infinity. Therefore, we can conclude that in this class of multi-serotype systems, the effects of ADE can cause a Hopf bifurcation for any number of serotypes. However, there is not much advantage in generating a large number of

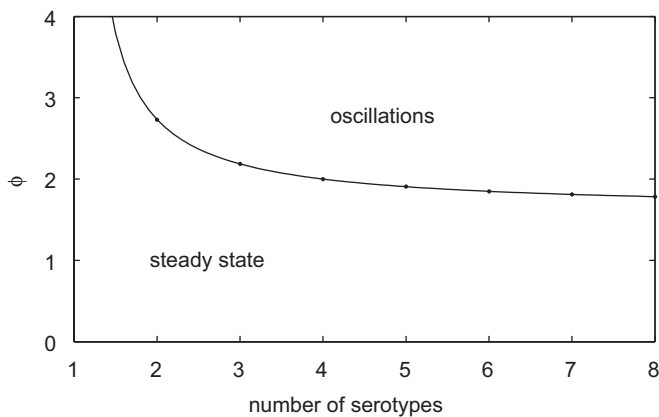


Fig. 5. The graph of Eq. (15) describing the Hopf bifurcation as a function of number of serotypes  $n$  and ADE factor  $\phi$ . Notice that as the number of serotypes increases, smaller ADE factors are needed for oscillatory dynamics.

serotypes if the goal is to lower the ADE factor necessary to induce oscillatory dynamics. Also, there is a balance between the number of co-circulating serotypes and the magnitude of ADE factors that do not induce oscillations that may threaten the persistence of each serotype (as discussed in Cummings et al., 2005).

### 5. Chaotic dynamics

Beyond the Hopf bifurcation, a common period doubling cascade leads to chaotic dynamics and serotype desynchronization. We turn to a Lyapunov exponent calculation to approximate the bifurcation value to chaos. We compute the maximum Lyapunov exponent by integrating the linear variational equations along solutions to the full model and using a time series of length  $t = 100,000$  years for a random initial condition, after transients are removed. Fig. 6 graphs these numerical approximations. The maximum exponent is negative for  $\phi < 1.883$ , which agrees with our stability analysis of the endemic equilibrium. The maximum exponent is approximately zero for  $1.883 < \phi < 1.91$ , which agrees with the periodic behavior after the Hopf bifurcation shown in Fig. 3. Chaotic behavior is indicated by a positive maximum Lyapunov exponent, which can be found for parameter values in the region  $\phi > 1.91$ .

For values of  $\phi$  just beyond the transition to chaos, the orbits gain and lose synchronization in a predictable pattern. A typical trajectory will oscillate with the variables synchronized by class within a slowly increasing envelope. Then, the variables unlock to separate phases for each serotype before possibly resynchronizing at a later time. We show a time series of all the secondary variables in Fig. 7 with a window of synchronous behavior.

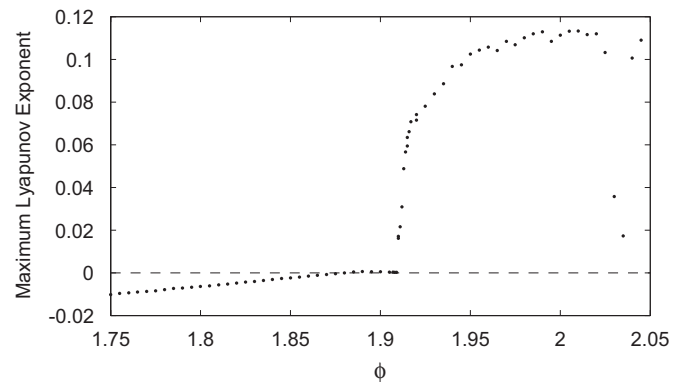


Fig. 6. A graph of the maximum Lyapunov exponent of Eq. (1) with  $n = 4$  as a function of  $\phi$ . We use a time series of length  $t = 100,000$  years for a random initial condition, after transients are removed.

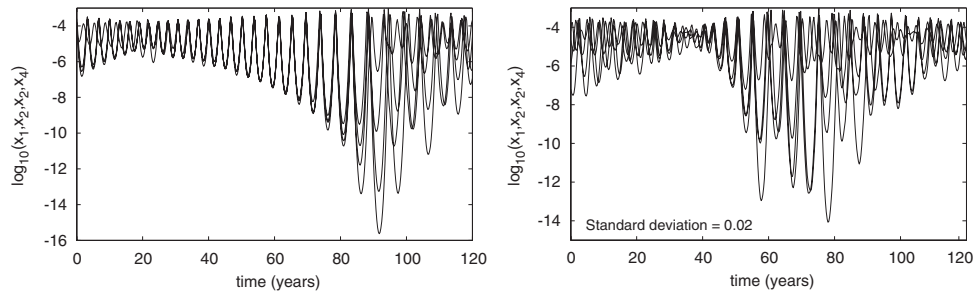


Fig. 7. On the left, a graph of a window of synchronous behavior for Eq. (1) with  $n = 4$  and  $\phi = 2.12$ . We plot  $\log_{10}$  of the primary infections as a function of time (years). On the right, the same plot with noise added at a standard deviation of 0.02. Notice the lack of long synchronous behavior before the lowest amplitude oscillations compared to the deterministic case on the left.

A numerical approximation of the Lyapunov exponents over the desynchronized regions indicates that trajectory is exhibiting chaotic behavior. As  $\phi$  increases, the trajectories spend more time exhibiting this unlocked behavior and we note the associated increase in the maximum Lyapunov exponent for the whole time series.

It is interesting to note that within each serotype, the maximum values of each primary and secondary infected time series remain synchronized for all  $\phi$ , and we only see a variation in amplitude. Across serotypes, we see phase differences that can reorder outbreaks in each burst group. In this parameter region, other behaviors are also possible. Synchronization can occur between two, three, or all four serotypes. As discussed in Cummings et al. (2005), synchronization can act in a boom-bust fashion, driving the numbers of infected individuals to greater extremes. If the percentage of infected individuals is sufficiently low, it could represent the fadeout of one or more serotypes.

## 6. Adding noise

We continue with an analysis of stochastic perturbations to the system in Eq. (1) to explore the robustness of solutions in this model to the effect of randomness. We add continuous multiplicative white noise to each of our disease state compartments, so that the randomness is proportional to the variable. Equivalently, we include additive noise in our numerical integration in the natural log space. The derivation of this equivalence follows.

Let  $\mathbf{Y} = \{s, x_i, r_i, x_{ij}\}_{i,j=1,\dots,n}$  and  $\dot{\mathbf{Y}} = F(\mathbf{Y})$ . Define natural log coordinates  $\mathbf{y} = \{y_i\}$ , where  $\ln(Y_i) = y_i$  (or  $Y_i = e^{y_i}$ ) and  $\dot{\mathbf{y}} = f(\mathbf{y})$ . Let  $\eta$  be a vector of random variables with mean zero and standard deviation  $\sigma$ . We add multiplicative noise to the original system in the following way:

$$\dot{Y}_i = F_i(\mathbf{Y}) + \eta_i Y_i. \quad (16)$$

Standard change of coordinates relates the two systems by  $\dot{Y}_i/Y_i = \dot{y}_i$ , so

$$\dot{Y}_i = Y_i f_i(\ln \mathbf{Y}) + \eta_i Y_i \quad (17)$$

and

$$\dot{\mathbf{y}} = f(\mathbf{y}) + \eta. \quad (18)$$

Eq. (18) was integrated numerically with additive noise using the Milstein method, which is a second order Runge–Kutta method for adding white noise to ordinary differential equations.

In Cummings et al. (2005), we reported that for stochastic perturbations with small standard deviations, fadeouts occur less frequently for values of  $\phi$  ranging from 2.0 to 2.5. We hypothesize that in this parameter range, the decrease is because noise breaks the synchrony of the solutions. Note that the typical behavior in the time series of the infected classes for the deterministic system with  $\phi$  in the range from 2.0 to 2.5 is a period of synchronous behavior between serotypes, with regular oscillations of spreading maximum/minimum amplitudes, followed by a period of asynchronous behavior, where one or more serotypes can experience fadeout dynamics. See the left graph in Fig. 7 as an example. The addition of noise in the system at these parameter values appears to keep the classes of components from becoming synchronized in phase and amplitude, so the fadeouts occur less frequently and without the precursor of synchronized oscillations, as shown in the right graph of Fig. 7.

We also note that in the larger parameter regions of  $\phi$ , the deterministic system does not typically undergo synchronization before fadeouts. In Cummings et al. (2005) we reported that for stochastic perturbations with small standard deviations, fadeouts occur more frequently for values of  $\phi$  between 2.5 and 3.0. Recall from the Hopf bifurcation analysis that the underlying unstable periodic orbits in the system have increasingly larger periods as we increase  $\phi$ . We hypothesize that the addition of noise could induce solutions to follow these paths for periods of time, with their extreme maximum/minimum amplitudes, and increase the occurrence of fadeouts.

## 7. Vaccinations

While a few candidate vaccines are under development, an effective licensed tetravalent vaccine against dengue will probably not be available for at least 5–10 years (CDC website, 2006). Though it is unclear whether successful vaccination against one serotype would place individuals at risk of severe disease in the same way that a natural

infection does, there is significant concern that this is the case. Therefore, vaccines that do not provide solid immunity to all four serotypes are not considered serious candidates for licensure (CDC website, 2006). However, it is clear that even in more advanced vaccines, there is concern that some vaccine failure might occur, potentially putting recipients at risk of severe disease upon exposure to serotypes from which vaccine-derived immunity not only does not protect, but enhances their infection.

Here, we consider the impact of vaccine failure in the extreme by considering the impact of a monotypic vaccine that grants full immunity to one serotype but does not grant immunity to the other three serotypes. As an example of this sort of vaccine, Steven Whitehead and colleagues at the Laboratory for Infectious Diseases, National Institutes of Health, Bethesda, Maryland have developed separate vaccine candidates for each of the four serotypes (Halstead et al., 2005). We assume that the immunity granted by this vaccine is similar to natural infection in its potential to provide antibody-dependent enhancement. However, we assume that one natural infection following vaccination is not sufficient to create immunity to all serotypes. Instead, individuals may become infected with two serotypes naturally following vaccination. Using our modeling framework, we compare the benefit of reducing one serotype in the population through vaccination to the potential increase in secondary infections due to the immunity granted to vaccine recipients.

To investigate the effects of implementing a single-serotype vaccination campaign, we assume that the entire population has been vaccinated against serotype four (arbitrarily chosen) and that it has 100% efficacy. Because there will be no infections of that serotype, we can remove the compartments associated with that serotype from the general model. The major difference in this model is that the force of infection by primary infected groups now includes the ADE factor. We write the general model in this compact form for  $i, j = 1, \dots, n - 1$ :

$$\begin{aligned} \frac{ds}{dt} &= \mu - s \sum_i \phi_i \beta_i \left( x_i + \sum_{j \neq i} x_{ji} \right) - \mu_d s, \\ \frac{dx_i}{dt} &= \phi_i \beta_i s \left( x_i + \sum_{j \neq i} x_{ji} \right) - \sigma x_i - \mu_d x_i, \\ \frac{dr_i}{dt} &= \sigma x_i - r_i \sum_{j \neq i} \phi_j \beta_j \left( x_j + \sum_{k \neq j} x_{kj} \right) - \mu_d r_i, \\ \frac{dx_{ij}}{dt} &= \phi_j \beta_j r_i \left( x_j + \sum_{k \neq j} x_{kj} \right) - \sigma x_{ij} - \mu_d x_{ij}. \end{aligned} \tag{19}$$

For  $\mu_d = \mu$ , the disease free equilibrium of Eq. (19) is similar to the non-vaccination model. The entire population is susceptible and all other compartments are empty. Again, its stability is determined by a basic reproduction number, or the maximum of the spectrum of the associated next generation matrix. We can define the basic reproduc-

tion number for each serotype as

$$\hat{R}_i = \frac{\beta_i \phi_i}{\mu + \sigma}, \tag{20}$$

resulting in a basic reproduction number for the system of  $\hat{R}_0 = \max_{i=1, \dots, n} \hat{R}_i$ . When  $\hat{R}_0 < 1$ , the disease free equilibrium is stable and the disease dies out.

As we increase  $\phi_i$ , the disease free equilibrium undergoes a transcritical bifurcation and exchanges stability with an endemic equilibrium. For the symmetric case of all  $\beta_i = \beta$  and  $\phi_i = \phi$ , the steady state is similar to the non-vaccination model in that when the endemic equilibrium is stable, the model dynamics are synchronized, or symmetric, with respect to serotype. In other words, all primary infectious, primary recovered, and secondary infectious variables equal within their own classes. Due to the vaccination, the reduced system for  $n$  serotypes now has  $n - 1$  serotypes, and the system can be generalized as

$$\begin{aligned} \frac{dz_1}{dt} &= \mu - (n - 1)\beta\phi z_1 z_2 - (n - 1)(n - 2)\beta\phi z_1 z_4 - \mu_d z_1, \\ \frac{dz_2}{dt} &= \beta\phi z_1 z_2 + (n - 2)\beta\phi z_1 z_4 - \sigma z_2 - \mu_d z_2, \\ \frac{dz_3}{dt} &= \sigma z_2 - (n - 2)\beta\phi z_3 z_2 - (n - 2)^2\beta\phi z_3 z_4 - \mu_d z_3, \\ \frac{dz_4}{dt} &= \beta\phi z_3 z_2 + (n - 2)\beta\phi z_3 z_4 - \sigma z_4 - \mu_d z_4. \end{aligned} \tag{21}$$

We can approximate the endemic equilibrium for the vaccinated system using the reduced non-mortality model ( $\mu_d = 0$ ):

$$\begin{aligned} (z_1, z_2, z_3, z_4) &= \left( \frac{\sigma}{2\beta\phi}, \frac{\mu}{(n - 1)\sigma}, \frac{\sigma}{2(n - 2)\beta\phi}, \frac{\mu}{(n - 1)(n - 2)\sigma} \right). \end{aligned} \tag{22}$$

For the parameters we have been addressing, we can show numerically by linearizing the system about this equilibrium that it is locally stable for  $1 \leq \phi \leq 5$ .

We would like to compare this full-vaccination model equilibrium to the equilibrium of the non-vaccination model (with no-mortality) from Eq. (9). In original parameters it has the form

$$\begin{aligned} (y_1, y_2, y_3, y_4) &= \left( \frac{\sigma}{\beta(\phi + 1)}, \frac{\mu}{n\sigma}, \frac{\sigma}{\beta(n - 1)(\phi + 1)}, \frac{\mu}{n(n - 1)\sigma} \right). \end{aligned} \tag{23}$$

While one could argue that the total number of infected are decreased in the vaccination model, since  $z_2 + z_4 < y_2 + y_4$ , we are interested in the total number of secondary infections, which has the higher incidence of the more severe form of dengue, DHF. Both infectious classes of the vaccination model are considered secondary, because the vaccination was equivalent to a primary infection. Therefore, we find  $y_4 < z_2 + z_4$  because  $0 < n^2 - 2n + 2$  for

all  $n \in \mathbb{R}$ , and conclude that single-serotype vaccinations could potentially increase the number of DHF cases for ADE values associated with an endemic steady-state in the non-vaccination model (before the Hopf bifurcation).

We note that single serotype vaccines have been tested in populations with no exposure to dengue and found to have 53–100% seroconversion rates (Sun et al., 2003). No single-serotype vaccines are being evaluated among persons at risk of exposure to dengue nor being designed for routine use because it is assumed that this would have a negative impact on health in any setting. Our quantitative model finds supporting evidence for this assumption.

## 8. Conclusions

In this paper, we have analyzed the dynamics of a multisero-type disease model with antibody-dependent enhancement. The model considered consists of compartments describing the fractions of susceptible, primary and secondary infectious, and recovered individuals. Although considered primarily for four serotypes and two sequential infections, the model is easily generalized to an arbitrary number of serotypes and infections.

We focus on the impact of the ADE parameter in the dynamics. Since ADE is modeled as an enhancement of mass action contacts in the secondary infectious rate, it is expected to play an important role in oscillatory onset of outbreaks. Indeed, we analyze quantitatively and numerically the sub-critical Hopf bifurcation from an endemic steady state to oscillatory dynamics. From the analysis, it is shown that the underlying period is quite sensitive to changes in ADE, and the window of parameter values for which stable periodic behavior occurs is quite small. A transition to chaotic, desynchronized behavior occurs for larger values of ADE and is robust over a very large range of parameter values, with occasional small windows of periodic behavior.

One interesting numerical finding is that there exist two distinct branches of periodic orbits which have slightly overlapping parameter values and which exhibit bi-stable solutions, as shown in Fig. 4. One branch occurs as a Hopf bifurcation, and the other branch appears as a saddle-node bifurcation. The stable branch of the saddle-node bifurcation has roughly 2.5 times the period of the Hopf branch. Since it is bi-stable over a small region, as ADE is changed, the dynamics may exhibit hysteresis, in which it switches from one type of behavior to another.

Beyond the range of ADE values exhibiting synchronized periodic dynamics, there exists a complicated set of chaotic oscillations, which is comprised of both synchronous and asynchronous outbreaks of the multiple serotypes. In the case where the dynamics is deterministic, synchronized behavior is in the form of an unstable focus, where the primary infectives grow in amplitude until some critical value, at which the infectives desynchronize and exhibit long period, large amplitude oscillations. It is possible that such synchronized behavior might be used to

predict a probability of fadeout of one or more serotypes. However, at present, there is no evidence in the data which points to such an indicator.

In addition to the deterministic case, we made a preliminary study of the effects of stochastic perturbations on the population. For small noise in the chaotic region, the dynamics exhibits asynchronous behavior most of the time, with similar increasing infectives as in the deterministic case. However, it is possible that stochastic perturbations can either increase or decrease the probability of fadeout, depending on the deterministic behavior of the system, as well as the ADE value.

Vaccination strategies need to be considered carefully to avoid an unintended effect. Since ADE is a function of secondary contact rates, the effect of vaccination on one serotype is expected to have a significant role in the asymptotic dynamics. If one vaccinates against a single serotype, the other infectious serotype classes all have contacts which are enhanced due to the ADE secondary infection hypothesis. In the endemic equilibrium, we showed that the total number of secondary cases is greater during the use of our modeled monotypic vaccination and conjecture that it is possible to potentially increase the number of secondary infections at steady state.

We hypothesize that the dynamics for some ADE parameter value greater than 1.91 (the onset of chaotic oscillations) could qualitatively agree with the Bangkok data reported in Nisalak et al. (2003). Vaccination schemes against all four serotypes can be tested with this model, and optimal strategies could be determined. Because of the sensitivity to the ADE parameter, we conclude that one would have to prove the strategy robust over a range of parameters, with and without stochastic perturbations. More detailed studies of vaccination strategies in this model are the subject of a future paper.

One interesting aspect of the multisero-type dynamics is the existence of very large fluctuations which lead to one or more serotypes possibly becoming extinct. Since the dynamics exhibits these large fluctuations in chaotic cases, there must be a large amplitude, long-period unstable orbit which attracts the dynamics by way of its stable manifold. For the unstable periodic orbits having long periods, it was seen that they also possess large amplitudes which, in the log variables, correspond to small fractions in the original “fraction” variables. Since the unstable orbits of long periods exist over almost all parameters of interest, it is quite possible they are the orbits which have a high probability of leading the dynamics to fadeout. Further studies involving the underlying unstable orbits will be studied in a future paper.

## Acknowledgments

L.B. and M.M. were supported by the National Science Foundation under Grants DMS-0414087 and CTS-0319555. L.B.S. and I.B.S. are supported by the Office of Naval Research, Center for Army Analysis, and the Armed

Forces Medical Intelligence Center. L.B.S. is currently a National Research Council post doctoral fellow. D.C. and D.B. were supported by the National Institute of General Medical Sciences of the National Institutes of Health Grant U01-GM070749-01 and a consortium of the National Oceanic and Atmospheric Administration, the Environmental Protection Agency, the National Aeronautics and Space Administration, and the National Science Foundation from Grant NA04OAR4310138.

## References

- Abu-Raddad, L.J., Ferguson, N.M., 2005. Characterizing the symmetric equilibrium of multi-strain host-pathogen systems in the presence of cross immunity. *J. Math. Biol.* 50, 531–558.
- Andreasen, V., Lin, J., Levin, S.A., 1997. The dynamics of cocirculating influenza strains conferring partial cross-immunity. *J. Math. Biol.* 35, 825–842.
- Burke, D.S., 1992. Human HIV vaccine trials: does antibody-dependent enhancement pose a genuine risk? *Perspect. Biol. Med.* 35, 511–530.
- Castillo-Chavez, C., Hethcote, H.W., Andreasen, V., Levin, S.A., Liu, W.M., 1989. Epidemiological models with age structure, proportionate mixing, and cross-immunity. *J. Math. Biol.* 27, 233–258.
- CDC website, 2006. (<http://www.cdc.gov/ncidod/dvbid/dengue/>).
- Cummings, D.A.T., Schwartz, I.B., Billings, L., Shaw, L.B., Burke, D.S., 2005. Dynamic effects of antibody dependent enhancement on the fitness of viruses. *Proc. Natl Acad. Sci. USA* 102, 15259–15264.
- Dawes, J.H.P., Gog, J.R., 2002. The onset of oscillatory dynamics in models of multistrain diseases. *J. Math. Biol.* 45, 471–510.
- Esteva, L., Vargas, C., 2000. Influence of vertical and mechanical transmission on the dynamics of dengue disease. *Math. Biosci.* 167, 51–64.
- Esteva, L., Vargas, C., 2003. Coexistence of different serotypes of dengue virus. *J. Math. Biol.* 46, 31–47.
- Ferguson, N.M., Anderson, R., Gupta, S., 1999a. The effect of antibody-dependent enhancement on the transmission dynamics and persistence of multiple-strain pathogens. *Proc. Natl Acad. Sci. USA* 96, 790–794.
- Ferguson, N.M., Donnelly, C.A., Anderson, R.M., 1999b. Transmission dynamics and epidemiology of dengue: insights from age-stratified sero-prevalence surveys. *Phil. Trans. R. Soc. London, Ser. B* 354, 757–768.
- Gubler, D.J., 1998. Dengue and dengue hemorrhagic fever. *Clin. Microbiol. Rev.* 11, 480–496.
- Halstead, S.B., Heinz, F.X., Barrett, A.D.T., Roehrig, J.T., 2005. Dengue virus: molecular basis of cell entry and pathogenesis, 25–27 June 2003, Vienna, Austria. *Vaccine* 23, 849–856.
- Nisalak, A., Endy, T.P., Nimmannitya, S., Kalayanarooj, S., Thisyakorn, U., Scott, R.M., Burke, D.S., Hoke, C.H., Innis, B.L., Vaughn, D.W., 2003. Serotype-specific dengue virus circulation and dengue disease in Bangkok, Thailand from 1973 to 1999. *Am. J. Trop. Med. Hyg.* 68, 191–202.
- Schwartz, I.B., Shaw, L.B., Cummings, D.A.T., Billings, L., McCrary, M., Burke, D., 2005. Chaotic desynchronization of multi-strain diseases. *Phys. Rev. E* 72, art. no. –066201.
- Sun, W., Edelman, R., Kanesa-Thanan, N., Eckels, K.H., Putnak, J.R., King, A.D., Houg, H.-S., Tang, D., Scherer, J.M., Hoke Jr., C.H., Innis, B.L., 2003. Vaccination of human volunteers with monovalent and tetravalent live-attenuated dengue vaccine candidates. *Am. J. Trop. Med. Hyg.* 69, 24–31.
- WHO website, 2006. (<http://www.who.int/mediacentre/factsheets/fs117/en/>).